ELSEVIER

Comput. Methods Appl. Mech. Engrg. 190 (2000) 1579–1599

Computer methods in applied mechanics and engineering

www.elsevier.com/locate/cma

Stabilization of incompressibility and convection through orthogonal sub-scales in finite element methods

Ramon Codina

Universitat Politècnica de Catalunya, Jordi Girona 1-3, Edifici C1, 08034 Barcelona, Spain

Received 15 April 1999; received in revised form 17 January 2000

Abstract

Two apparently different forms of dealing with the numerical instability due to the incompressibility constraint of the Stokes problem are analyzed in this paper. The first of them is the stabilization through the pressure gradient projection, which consists of adding a certain least-squares form of the difference between the pressure gradient and its L^2 projection onto the discrete velocity space in the variational equations of the problem. The second is a sub-grid scale method, whose stabilization effect is very similar to that of the Galerkin/least-squares (GLS) method for the Stokes problem. It is shown here that the first method can also be recast in the framework of sub-grid scale methods with a particular choice for the space of sub-scales. This leads to a new stabilization procedure, whose applicability to stabilize convection is also studied in this paper.

1. Introduction

One of the most important problems in computational mechanics is the treatment of the incompressibility. Even though this problem is well understood and there are several ways to deal with it, it is still a subject of active research, mainly because incompressible situations appear both in solid and in fluid mechanics together with other phenomena that are also sources of numerical instabilities. A general stabilization technique applicable to all these problems in still missing, and the incompressibility is revisited every time a new stabilization method is proposed.

The objective of this paper is to analyze a stabilized finite element method originally designed for the Stokes problem. However, rather than introducing a *new* method, the first goal is to recast *existing* methods in a general framework. More precisely, it is shown here how the method presented in [1], based on the pressure gradient projection, can be understood as a sub-grid scale method as introduced for scalar equations in [2] and applied to systems of convection–diffusion–reaction equations in [3].

This abstraction allows one to go further and to consider the possibility of stabilizing other classical sources of numerical instabilities, such as convection with low diffusive terms, using the same ideas. This possibility is also investigated in this paper. However, the starting point will be the Stokes problem, which can be written as

$$-\nu\Delta\boldsymbol{u}+\nabla p=\boldsymbol{f}\quad\text{in }\Omega, \tag{1}$$

$$\nabla\cdot\boldsymbol{u}=0\quad\text{in }\Omega, \tag{2}$$

E-mail address: ramon.codina@upc.es (R. Codina).

0045-7825/00/$ - see front matter
PII: S0045-7825(00)00254-1

where $\boldsymbol{u}$ is the displacement in an elasticity problem or the velocity field in a creeping flow problem, p the pressure, ν the shear modulus or the viscosity, depending on the problem, $\boldsymbol{f}$ the vector of body forces and Ω is the computational domain. For the sake of simplicity, the simplest Dirichlet condition

$$\boldsymbol{u} = \boldsymbol{0} \quad \text{on } \partial\Omega,$$

will be considered throughout in the paper.

Let us introduce now some notation. As usual, the space of square integrable functions in a domain Ω is denoted by $L^2(\Omega)$, and the space of functions whose distributional derivatives of order up to $m \geqslant 0$ (integer) belong to $L^2(\Omega)$ by $H^m(\Omega)$. The space $H_0^1(\Omega)$ consists of functions in $H^1(\Omega)$ vanishing on $\partial\Omega$. A bold character is used to denote the vector counterpart of these spaces. The L^2 inner product in Ω is denoted by $(\cdot,\cdot)$ and the associated norm by $\|\cdot\|$.

Using this notation, the velocity and pressure finite element spaces for the continuous problem are

$$\mathscr{V}_0 = \boldsymbol{H}_0^1(\Omega), \quad \mathscr{Q} = \left\{ q \in L^2(\Omega) \,\middle|\, \int_\Omega q \,\mathrm{d}\Omega = 0 \right\}.$$

The variational statement for problems (1) and (2) can be written in terms of the bilinear forms

$$a(\boldsymbol{u},\boldsymbol{v}) = \nu(\nabla\boldsymbol{u},\nabla\boldsymbol{v}), \quad b(q,\boldsymbol{v}) = (q,\nabla\cdot\boldsymbol{v}),$$

where $\boldsymbol{u},\boldsymbol{v} \in \mathscr{V}_0$ and $q \in \mathscr{Q}$.

Having introduced this notation, the variational form of the problem reads: find $(\boldsymbol{u},p) \in \mathscr{V}_0 \times \mathscr{Q}$ such that

$$a(\boldsymbol{u},\boldsymbol{v}) - b(p,\boldsymbol{v}) = (\boldsymbol{f},\boldsymbol{v}) \quad \forall \boldsymbol{v} \in \mathscr{V}_0,$$
$$b(q,\boldsymbol{u}) = 0 \quad \forall q \in \mathscr{Q}.$$

For simplicity, we have assumed that the components of $\boldsymbol{f}$ are in $L^2(\Omega)$.

The well-posedness of this problem relies on the coercivity of the bilinear form a and the inf–sup or Babuška–Brezzi condition (see [4]), which can be shown to hold for the continuous problem. The first property is automatically inherited by its discrete counterpart, which can be written as: find $(\boldsymbol{u}_h,p_h) \in \mathscr{V}_{h,0} \times \mathscr{Q}_h$ such that

$$a(\boldsymbol{u}_h,\boldsymbol{v}_h) - b(p_h,\boldsymbol{v}_h) = (\boldsymbol{f},\boldsymbol{v}_h) \quad \forall \boldsymbol{v}_h \in \mathscr{V}_{h,0}, \tag{3}$$
$$b(q_h,\boldsymbol{u}_h) = 0 \quad \forall q_h \in \mathscr{Q}_h, \tag{4}$$

where $\mathscr{V}_{h,0}$ and $\mathscr{Q}_h$ are the finite element spaces for the velocity and the pressure. However, the inf–sup condition needs to be explicitly required. This leads to the need of using mixed interpolations, that is, different for $\boldsymbol{u}$ and p.

The objective of stabilized finite element formulations for the Stokes problem is to modify conveniently problems (3) and (4) so as to end up with a method for which the Babuška–Brezzi condition is not necessary and, in particular, equal velocity–pressure interpolations are possible. Moreover, the resulting formulation must be able to be extended to cases with skew symmetric terms in $a(\boldsymbol{u},\boldsymbol{v})$ (such as convective terms or Coriolis forces), which may lead to numerical instabilities (see [5] for a description of the numerical problems encountered when the Coriolis force dominates).

In the next section, one of such stabilized formulations is described. This method was presented in [1] and is briefly recalled here. In Section 3 an apparently different method is also described. This method is based on the sub-grid scale concept [2] and, for the Stokes problem, is very similar to the Galerkin/least-squares (GLS) method (see e.g. [6]). Once the two finite element formulations have been fully described, Section 4 is devoted to show the connection between both, which is one of the main objectives of this paper. It is shown in that section that the method of Section 2 corresponds to a particular choice for the space of sub-scales, called here *space of orthogonal sub-scales*. The next step is to apply this idea to a different problem with a different type of numerical instability, such as the convection–diffusion–reaction equation in the case of small diffusion. This is done in Section 5. Some numerical examples are presented in Section 6, and the paper concludes with the summary of the most important results in Section 7.

2. Stabilization of the Stokes problem I: the pressure gradient projection

In this section we briefly recall the stabilized formulation presented in [1], which in turn has as main motivation to recover the stabilization effect of some fractional step methods, as described in what follows.

2.1. Motivation: on a class of fractional step methods

Let us consider the transient Stokes problem:

$$\frac{\partial \boldsymbol{u}}{\partial t} - \nu \Delta \boldsymbol{u} + \nabla p = \boldsymbol{f},$$
$$\nabla \cdot \boldsymbol{u} = 0$$

supplied with suitable initial and boundary conditions.

Let us consider also a partition of the time interval with time step size δt. If $\boldsymbol{u}^n$ is a known approximation to $\boldsymbol{u}$ at time step n, the classical fractional step or projection method applied to this problem [7,8] consists of finding $\boldsymbol{u}^{n+1/2}$, $\boldsymbol{u}^{n+1}$ and p^{n+1} as the solution to the problem:

$$\frac{1}{\delta t}\left(\boldsymbol{u}^{n+1/2} - \boldsymbol{u}^n\right) - \nu \Delta \boldsymbol{u}^{n+1/2} = \boldsymbol{f}, \tag{5}$$
$$\frac{1}{\delta t}\left(\boldsymbol{u}^{n+1} - \boldsymbol{u}^{n+1/2}\right) + \nabla p^{n+1} = \boldsymbol{0}, \tag{6}$$
$$\nabla \cdot \boldsymbol{u}^{n+1} = 0, \tag{7}$$

with appropriate boundary conditions that are irrelevant for this discussion.

To uncouple (6) and (7) it is convenient to take the divergence of the first equation, which yields

$$\Delta p^{n+1} = \frac{1}{\delta t} \nabla \cdot \boldsymbol{u}^{n+1/2}. \tag{8}$$

Once the finite element discretization has been performed, the discrete matrix form of the previous equations is

$$\frac{1}{\delta t}\mathbf{M}\left(\mathbf{U}^{n+1/2} - \mathbf{U}^n\right) + \mathbf{K}\mathbf{U}^{n+1/2} = \mathbf{F}, \tag{9}$$
$$\frac{1}{\delta t}\mathbf{M}\left(\mathbf{U}^{n+1} - \mathbf{U}^{n+1/2}\right) + \mathbf{G}\mathbf{P}^{n+1} = \mathbf{0}, \tag{10}$$
$$-\mathbf{G}^{\mathrm{t}}\mathbf{U}^{n+1} = \mathbf{0}, \tag{11}$$
$$\delta t\,\mathbf{L}\mathbf{P}^{n+1} - \mathbf{G}^{\mathrm{t}}\mathbf{U}^{n+1/2} = \mathbf{0}, \tag{12}$$

where capital letters $\mathbf{U}$ and $\mathbf{P}$ denote the vectors of velocity and pressure nodal unknowns and $\mathbf{M}$, $\mathbf{K}$, $\mathbf{G}$ and $\mathbf{L}$ are the matrices coming from the temporal, viscous, gradient and Laplacian terms, respectively.

From (10) and (12) it is found that

$$-\mathbf{G}^{\mathrm{t}}\mathbf{U}^{n+1} + \delta t\left(\mathbf{L} - \mathbf{G}^{\mathrm{t}}\mathbf{M}^{-1}\mathbf{G}\right)\mathbf{P}^{n+1} = \mathbf{0}, \tag{13}$$

which is obviously different from (11). Therefore, it is seen that whereas at the continuous level (5) + (6) + (7) = (5) + (8) + (6), at the discrete level (9) + (10) + (11) ≠ (9) + (12) + (10). The continuity equation has been modified to the *stabilized equation* (13). This fact was observed in [9] and is the reason why this type of fractional step methods allow us to use equal velocity–pressure interpolations.

Remark 1. The approach followed here and in [1] has been used to analyze the stabilization introduced by the use of the Poisson equation (8) *on the end-of-step velocity*. However, in [10] it was shown that the problem can be considered as a stabilized one *for the intermediate velocity*, with a stabilization effect similar to that of the GLS method.

2.2. Stabilized finite element formulation

Let us consider now the stationary problem. In order to recover the previous stabilization effect, problems (3) and (4) can be modified to:

$$a(\boldsymbol{u}_h, \boldsymbol{v}_h) - b(p_h, \boldsymbol{v}_h) = (\boldsymbol{f}, \boldsymbol{v}_h) \quad \forall \boldsymbol{v}_h \in \mathscr{V}_{h,0}, \tag{14}$$

$$\alpha(\nabla p_h, \nabla q_h) - \alpha(\boldsymbol{\xi}_h, \nabla q_h) + b(q_h, \boldsymbol{u}_h) = 0 \quad \forall q_h \in \mathscr{Q}_h, \tag{15}$$

$$-(\nabla p_h, \boldsymbol{\eta}_h) + (\boldsymbol{\xi}_h, \boldsymbol{\eta}_h) = 0 \quad \forall \boldsymbol{\eta}_h \in \mathscr{V}_h, \tag{16}$$

where $\alpha > 0$ is a given numerical parameter and $\mathscr{V}_h$ is the velocity space *without boundary conditions* (that is, the finite element space to approximate $\boldsymbol{H}^1(\Omega)$). It is observed from (16) that $\boldsymbol{\xi}_h$ is the L^2 projection of ∇p_h onto $\mathscr{V}_h$.

The matrix form of (14)–(16) is

$$\mathbf{K}\mathbf{U} + \mathbf{G}_0\mathbf{P} = \mathbf{F}_0, \tag{17}$$

$$\alpha\mathbf{L}\mathbf{P} - \alpha\mathbf{G}^{\mathrm{t}}\boldsymbol{\Xi} - \mathbf{G}_0^{\mathrm{t}}\mathbf{U} = \mathbf{0}, \tag{18}$$

$$-\mathbf{G}\mathbf{P} + \mathbf{M}\boldsymbol{\Xi} = \mathbf{0}, \tag{19}$$

where subscript 0 accounts for the Dirichlet boundary conditions. If $\boldsymbol{\Xi}$ is eliminated from (18) using (19) it is seen that the continuity equation associated to this method is

$$\alpha\left(\mathbf{L} - \mathbf{G}^{\mathrm{t}}\mathbf{M}^{-1}\mathbf{G}\right)\mathbf{P} - \mathbf{G}_0^{\mathrm{t}}\mathbf{U} = \mathbf{0},$$

which is very similar to (13).

2.3. Stability

Although it is not the purpose of this section to repeat the stability analysis presented in [1], it is essential to introduce the basic ideas of this analysis in the following.

Consider the space

$$\mathscr{E}_h := \mathscr{V}_h + \nabla\mathscr{Q}_h = \mathscr{E}_{h,1} \oplus \mathscr{E}_{h,2} \oplus \mathscr{E}_{h,3},$$

where $\mathscr{E}_{h,i}$, $i = 1, 2, 3$, are three mutually L^2 orthogonal sub-spaces defined as

$$\mathscr{E}_{h,1} := \mathscr{V}_{h,0},$$

$$\mathscr{E}_{h,2} := \mathscr{V}_{h,0}^{\perp} \cap \mathscr{V}_h,$$

$$\mathscr{E}_{h,3} := \mathscr{V}_h^{\perp}.$$

Let $P_{h,i}$ be the orthogonal projection from $\mathscr{E}_h$ *to* $\mathscr{E}_{h,i}$, $P_{h,ij} := P_{h,i} + P_{h,j}$, $i, j = 1, 2, 3$ and $\mathscr{E}_{h,ij} := \mathscr{E}_{h,i} \oplus \mathscr{E}_{h,j}$. The way to show that the pressure solution of problems (14)–(16) is stable is to decompose its gradient as

$$\nabla p_h = P_{h,1}(\nabla p_h) + P_{h,2}(\nabla p_h) + P_{h,3}(\nabla p_h).$$

As shown in [1], stability for $P_{h,1}(\nabla p_h)$ can be obtained from the momentum equation, for $P_{h,3}(\nabla p_h)$ it is provided by the new terms added to the Galerkin ones (those involving the parameter α) and, finally, control over $P_{h,2}(\nabla p_h)$ needs to be explicitly required through the weakened inf–sup condition

$$\inf_{q_h \in \mathscr{Q}_h} \sup_{\boldsymbol{v}_h \in \mathscr{E}_{h,13}} \frac{(\nabla q_h, \boldsymbol{v}_h)}{\|\nabla q_h\| \|\boldsymbol{v}_h\|} \geqslant C > 0. \tag{20}$$

This condition is similar to the classical Babuška–Brezzi one but easier to satisfy (observe that the space where $\boldsymbol{v}_h$ runs is larger than for the classical inf–sup condition). In particular, it can be shown that equal interpolations satisfy it.

Let h be the element size of a quasi-uniform finite element partition. The following result gives the stability estimate for the solution to problems (14)–(16).

Theorem 1. *Suppose that the family of finite element partitions is quasi-uniform and the weakened inf–sup condition holds. If $\alpha \geqslant \alpha_0 h^2$ for a constant α_0, there exists a unique solution to the discrete problem that verifies the stability estimate*

$$\|\nabla \boldsymbol{u}_h\| + h\|\nabla p_h\| \leqslant C\|\boldsymbol{f}\| \tag{21}$$

for a constant C independent of h.

Remark 2. Condition $\alpha \geqslant \alpha_0 h^2$ needs to be replaced by $\alpha_1 h^2 \geqslant \alpha \geqslant \alpha_0 h^2$ to prove convergence (with α_1 a constant), that is, α *must* be of order $O(h^2)$. The convergence estimates proved in [1] are *optimal*, both in the norm defined by the left-hand side of (21) and in L^2 norms of the velocity and the pressure. The proof-technique is similar to that used in Section 5 for the convection–diffusion equation.

3. Stabilization of the Stokes problem II: sub-grid scale methods

3.1. Model problem

Let us discuss now an apparently different stabilization technique, which later on will be shown to be related to that of the previous section.

Let us start taking as model problem the system of convection–diffusion–reaction equations

$$\mathscr{L}(\boldsymbol{U}) := \frac{\partial}{\partial x_i}(\boldsymbol{A}_i \boldsymbol{U}) - \frac{\partial}{\partial x_i}\left(\boldsymbol{K}_{ij}\frac{\partial \boldsymbol{U}}{\partial x_i}\right) + \boldsymbol{S}\boldsymbol{U} = \boldsymbol{F} \quad \text{in } \Omega, \tag{22}$$

$$\boldsymbol{U} = \boldsymbol{0} \quad \text{on } \partial\Omega, \tag{23}$$

where $\boldsymbol{U}$ and $\boldsymbol{F}$ are vectors of n_{unk} unknowns and $\boldsymbol{A}_i$, $\boldsymbol{K}_{ij}$ and $\boldsymbol{S}$ are $n_{\text{unk}} \times n_{\text{unk}}$ matrices ($i, j = 1, \ldots, n_{\text{sd}}$, the number of space dimensions).

For simplicity, assume that the algebraic bilinear form associated to $\boldsymbol{K}_{ij}$ is positive definite. Let $\mathscr{W} := (H^1(\Omega))^{n_{\text{unk}}}$, $\mathscr{W}_0 = (H_0^1(\Omega))^{n_{\text{unk}}}$. The weak form of the problem is: find $\boldsymbol{U} \in \mathscr{W}_0$ such that

$$B(\boldsymbol{U}, \boldsymbol{V}) = L(\boldsymbol{V}) \quad \forall \boldsymbol{V} \in \mathscr{W}_0,$$

where

$$B(\boldsymbol{U}, \boldsymbol{V}) := \int_\Omega \boldsymbol{V}^{\mathrm{t}} \frac{\partial}{\partial x_i}(\boldsymbol{A}_i \boldsymbol{U})\,\mathrm{d}\Omega + \int_\Omega \frac{\partial \boldsymbol{V}^{\mathrm{t}}}{\partial x_i}\boldsymbol{K}_{ij}\frac{\partial \boldsymbol{U}}{\partial x_j}\,\mathrm{d}\Omega + \int_\Omega \boldsymbol{V}^{\mathrm{t}}\boldsymbol{S}\boldsymbol{U}\,\mathrm{d}\Omega,$$

$$L(\boldsymbol{V}) := \int_\Omega \boldsymbol{V}^{\mathrm{t}}\boldsymbol{F}\,\mathrm{d}\Omega.$$

The Galerkin finite element approximation is straightforward. If $\mathscr{W}_h$ is a finite element approximation to $\mathscr{W}$ and $\mathscr{W}_{h,0}$ to $\mathscr{W}_0$, the problem is: find $\boldsymbol{U}_h \in \mathscr{W}_{h,0}$ such that

$$B(\boldsymbol{U}_h, \boldsymbol{V}_h) = L(\boldsymbol{V}_h) \quad \forall \boldsymbol{V}_h \in \mathscr{W}_{h,0}. \tag{24}$$

3.2. The sub-grid scale approach

It is well known that the Galerkin approximation (24) may suffer from several instability problems. In order to overcome them, we present in the following the sub-grid scale concept, originally presented for scalar equations in [2] and extended to systems in [3].

3.2.1. Description of the method

Let $\mathscr{W} = \mathscr{W}_h \oplus \tilde{\mathscr{W}}$, where $\tilde{\mathscr{W}}$ is any space to complete $\mathscr{W}_h$ in $\mathscr{W}$. To avoid technicalities, we may think of $\mathscr{W}$ and $\tilde{\mathscr{W}}$ as finite dimensional, with a large dimension. Likewise, let $\mathscr{W}_0 = \mathscr{W}_{h,0} \oplus \tilde{\mathscr{W}}_0$, with $\tilde{\mathscr{W}}_0$ any complement of $\mathscr{W}_{h,0}$ in $\mathscr{W}_0$.

The continuous problem is equivalent to

$$B(\boldsymbol{U}_h, \boldsymbol{V}_h) + B(\tilde{\boldsymbol{U}}, \boldsymbol{V}_h) = L(\boldsymbol{V}_h) \quad \forall \boldsymbol{V}_h \in \mathscr{W}_{h,0}, \tag{25}$$

$$B(\boldsymbol{U}_h, \tilde{\boldsymbol{V}}) + B(\tilde{\boldsymbol{U}}, \tilde{\boldsymbol{V}}) = L(\tilde{\boldsymbol{V}}) \quad \forall \tilde{\boldsymbol{V}} \in \tilde{\mathscr{W}}_0, \tag{26}$$

where $\boldsymbol{U} = \boldsymbol{U}_h + \tilde{\boldsymbol{U}}$ and $\boldsymbol{U}_h \in \mathscr{W}_{h,0}$, $\tilde{\boldsymbol{U}} \in \tilde{\mathscr{W}}_0$. Let n_{el} be the number of elements of the finite element partition. Introducing the notation

$$\int_{\Omega'} := \sum_{e=1}^{n_{\mathrm{el}}} \int_{\Omega^e}, \quad \int_{\partial\Omega'} := \sum_{e=1}^{n_{\mathrm{el}}} \int_{\partial\Omega^e},$$

and integrating by parts within each element in (25) and (26), it is found that these two equations can be written as:

$$B(\boldsymbol{U}_h, \boldsymbol{V}_h) + \int_{\partial\Omega'} \tilde{\boldsymbol{U}}^{\mathrm{t}} n_i \boldsymbol{K}_{ij} \frac{\partial \boldsymbol{V}_h}{\partial x_j} \,\mathrm{d}\Gamma + \int_{\Omega'} \tilde{\boldsymbol{U}}^{\mathrm{t}} \mathscr{L}^*(\boldsymbol{V}_h) \,\mathrm{d}\Omega = L(\boldsymbol{V}_h), \tag{27}$$

$$\int_{\partial\Omega'} \tilde{\boldsymbol{V}}^{\mathrm{t}} n_i \boldsymbol{K}_{ij} \frac{\partial}{\partial x_j}(\boldsymbol{U}_h + \tilde{\boldsymbol{U}}) \,\mathrm{d}\Gamma + \int_{\Omega'} \tilde{\boldsymbol{V}}^{\mathrm{t}} \mathscr{L}(\tilde{\boldsymbol{U}}) \,\mathrm{d}\Omega = \int_{\Omega'} \tilde{\boldsymbol{V}}^{\mathrm{t}} [\boldsymbol{F} - \mathscr{L}(\boldsymbol{U}_h)] \,\mathrm{d}\Omega, \tag{28}$$

where $\mathscr{L}^*$ is the formal adjoint of $\mathscr{L}$. Since diffusive fluxes must be continuous across inter-element boundaries, the first term of (28) vanishes. This equation is equivalent to:

$$\mathscr{L}(\tilde{\boldsymbol{U}}) = \boldsymbol{F} - \mathscr{L}(\boldsymbol{U}_h) + \boldsymbol{V}_{h,\mathrm{ort}} \quad \text{in } \Omega^e \ \forall \boldsymbol{V}_{h,\mathrm{ort}} \in \tilde{\mathscr{W}}_0^{\perp}, \tag{29}$$

$$\tilde{\boldsymbol{U}} = \tilde{\boldsymbol{U}}_{\mathrm{ske}} \quad \text{on } \partial\Omega^e, \tag{30}$$

for $e = 1, \ldots, n_{\mathrm{el}}$ and for a certain function $\tilde{\boldsymbol{U}}_{\mathrm{ske}}$ that we call the *skeleton* of $\boldsymbol{U}$. It is important to remark that (29) holds for any element $\boldsymbol{V}_{h,\mathrm{ort}}$ orthogonal to $\tilde{\mathscr{W}}_0$.

Up to now, no approximation has been introduced. The questions now are:

- How to choose $\boldsymbol{V}_{h,\mathrm{ort}}$?
- How to approximate $\tilde{\boldsymbol{U}}_{\mathrm{ske}}$?
- How to solve for $\tilde{\boldsymbol{U}}$?

3.2.2. Algebraic approximation to the sub-scales

This is the simplest answer to the previous questions. First of all $\tilde{\mathscr{W}}_0$ is taken as a space of *bubble functions*, that is, vanishing on the boundaries of the elements (see [11,12]). This means that $\tilde{\boldsymbol{U}}_{\mathrm{ske}} = \boldsymbol{0}$. The function $\boldsymbol{V}_{h,\mathrm{ort}}$ is also taken as $\boldsymbol{0}$ (recall that (29) was obtained from (28).

It only remains to solve for $\tilde{\boldsymbol{U}}$ in (29), now in the space of bubble functions. A simple approximation, which can be motivated by approximating the effect of $\tilde{\boldsymbol{U}}$ in (27), is

$$\tilde{\boldsymbol{U}} \approx \boldsymbol{\tau}[\boldsymbol{F} - \mathscr{L}(\boldsymbol{U}_h)], \tag{31}$$

where $\boldsymbol{\tau}$ is a $n_{\mathrm{unk}} \times n_{\mathrm{unk}}$ matrix defined within each element domain and referred to as the *matrix of stabilization parameters*.

The final problem to be solved is

$$B(\boldsymbol{U}_h, \boldsymbol{V}_h) + \int_{\Omega'} \tilde{\boldsymbol{U}}^{\mathrm{t}} \mathscr{L}^*(\boldsymbol{V}_h) \,\mathrm{d}\Omega = L(\boldsymbol{V}_h), \tag{32}$$

where $\tilde{\boldsymbol{U}}$ is given by (31) and the adjoint of the convection–diffusion–reaction operator is

$$\mathscr{L}^*(\boldsymbol{V}_h) = -\boldsymbol{A}_i^{\mathrm{t}} \frac{\partial \boldsymbol{V}_h}{\partial x_i} - \frac{\partial}{\partial x_i}\left(\boldsymbol{K}_{ij}^{\mathrm{t}} \frac{\partial \boldsymbol{V}_h}{\partial x_j}\right) + \boldsymbol{S}^{\mathrm{t}} \boldsymbol{V}_h. \tag{33}$$

3.3. Application to the Stokes problem

To simplify the notation, let us consider the 2D case. The Stokes problem can be written in the form (22), now with

$$\boldsymbol{A}_1 = \begin{bmatrix} 0 & 0 & 1 \\ 0 & 0 & 0 \\ 1 & 0 & 0 \end{bmatrix}, \quad \boldsymbol{A}_2 = \begin{bmatrix} 0 & 0 & 0 \\ 0 & 0 & 1 \\ 0 & 1 & 0 \end{bmatrix}, \quad \boldsymbol{K}_{ii} = \begin{bmatrix} \nu & 0 & 0 \\ 0 & \nu & 0 \\ 0 & 0 & 0 \end{bmatrix},$$

for $i = 1, 2$, and $\boldsymbol{S} = \boldsymbol{K}_{12} = \boldsymbol{K}_{21} = \boldsymbol{0}$. The algebraic bilinear form associated to $\boldsymbol{K}_{ij}$ is only positive semi-definite in this case, but the previous development is applicable now as well.

Let $\boldsymbol{U}_h = [u_{1,h}, u_{2,h}, p_h]^{\mathrm{t}}$, $\boldsymbol{V}_h = [v_{1,h}, v_{2,h}, q_h]^{\mathrm{t}}$ and $\mathscr{W}_{h,0} = \mathscr{V}_{h,0} \times \mathscr{Q}_h$. The bilinear form associated to the problem is

$$B(\boldsymbol{U}_h, \boldsymbol{V}_h) = \nu \int_\Omega \nabla \boldsymbol{u}_h : \nabla \boldsymbol{v}_h \, \mathrm{d}\Omega - \int_\Omega p_h \nabla \cdot \boldsymbol{v}_h \, \mathrm{d}\Omega + \int_\Omega q_h \nabla \cdot \boldsymbol{u}_h \, \mathrm{d}\Omega.$$

Taking $\boldsymbol{v}_h = \boldsymbol{u}_h$ and $p_h = q_h$ it is found that

$$B(\boldsymbol{U}_h, \boldsymbol{U}_h) = \nu \|\nabla \boldsymbol{u}_h\|^2.$$

It is seen that the pressure is out of control. This is why the discrete inf–sup condition is needed.

The adjoint of the operator $\mathscr{L}$ in this case is

$$\mathscr{L}^*(\boldsymbol{V}_h) = \begin{bmatrix} -\nu \Delta \boldsymbol{v}_h - \nabla q_h \\ -\nabla \cdot \boldsymbol{v}_h \end{bmatrix}.$$

The problem is how to take the matrix of stabilization parameters. For this particular case it can be shown that

$$\boldsymbol{\tau} = \mathrm{diag}(\tau_1, \tau_1, \tau_2) \tag{34}$$

is effective. The resulting stabilizing term is then

$$-\int_{\Omega'} \mathscr{L}^*(\boldsymbol{V}_h)^{\mathrm{t}} \boldsymbol{\tau} \mathscr{L}(\boldsymbol{U}_h) \, \mathrm{d}\Omega = \int_{\Omega'} \tau_1 (\nu \Delta \boldsymbol{v}_h + \nabla q_h) \cdot (-\nu \Delta \boldsymbol{u}_h + \nabla p_h) \, \mathrm{d}\Omega + \int_{\Omega'} \tau_2 (\nabla \cdot \boldsymbol{v}_h)(\nabla \cdot \boldsymbol{u}_h) \, \mathrm{d}\Omega.$$

The convergence analysis of this method (see [13]) shows that the parameters τ_1 and τ_2 can be taken as

$$\tau_1 = \left(\frac{c_1 \nu}{h^2} \right)^{-1}, \quad \tau_2 = c_2 \frac{h^2}{\tau_1},$$

where c_1 and c_2 are numerical constants. This completes the definition of the stabilization method.

Remark 3. It is interesting to note that if the incompressibility condition (6) is penalized, that is, it is substituted by $\varepsilon p + \nabla \cdot \boldsymbol{u} = 0$, the simple diagonal expression (34) for $\boldsymbol{\tau}$ is not enough, unless the penalty parameter ε is sufficiently small. It turns out that the precise condition on ε is similar to that which ensures convergence of augmented Lagrangian methods, as analyzed in [14].

4. The link between I and II

In this section it is shown that the stabilization technique presented in Section 2 can be recast in the framework of sub-grid scale methods described in the previous section. First, a general concept is introduced, which will allow us to make this identification. This general concept is applied in Section 5 to stabilize convection.

4.1. Orthogonal sub-scales

Recall that the basic decomposition of the sub-grid scale method is to take $\mathscr{W} = \mathscr{W}_h \oplus \tilde{\mathscr{W}}$ and $\mathscr{W}_0 = \mathscr{W}_{h,0} \oplus \tilde{\mathscr{W}}_0$ and that the problem for the sub-scales is (29) and (30). If $\cong$ denotes an isomorphism between two vector spaces, what we always have is that

$$\mathscr{W} = \mathscr{W}_h \oplus \tilde{\mathscr{W}}, \quad \tilde{\mathscr{W}} \cong \mathscr{W}_h^{\perp} \cap (H^1(\Omega))^{n_{\mathrm{unk}}},$$
$$\mathscr{W}_0 = \mathscr{W}_{h,0} \oplus \tilde{\mathscr{W}}_0, \quad \tilde{\mathscr{W}}_0 \cong \mathscr{W}_{h,0}^{\perp} \cap (H_0^1(\Omega))^{n_{\mathrm{unk}}}.$$

The election of $\tilde{\mathscr{W}}$ and $\tilde{\mathscr{W}}_0$ is still open. A legitimate choice is to take

$$\tilde{\mathscr{W}} = \mathscr{W}_h^{\perp} \cap (H^1(\Omega))^{n_{\mathrm{unk}}}. \tag{35}$$

To obtain a feasible numerical method we need to introduce some approximations. The first concerns the choice for $\tilde{\mathscr{W}}_0$. First, we assume that functions in $\tilde{\mathscr{W}}$ already vanish on $\partial\Omega$, and thus $\tilde{\mathscr{W}}_0 \approx \tilde{\mathscr{W}}$. Additionally we assume that $\mathscr{W}_h^{\perp} \cap (H^1(\Omega))^{n_{\mathrm{unk}}} \approx \mathscr{W}_h^{\perp}$, which can be thought of as a non-conforming approximation for the sub-scales. Altogether, this amounts to saying that

$$\tilde{\mathscr{W}}_0 \approx \tilde{\mathscr{W}} \approx \mathscr{W}_h^{\perp}. \tag{36}$$

With this approximation, it follows from (29) that

$$\boldsymbol{V}_{h,\mathrm{ort}} \in \tilde{\mathscr{W}}_0^{\perp} \approx \mathscr{W}_h, \tag{37}$$
$$\tilde{\boldsymbol{U}} \in \tilde{\mathscr{W}}_0 \approx \mathscr{W}_h^{\perp}, \tag{38}$$

which means that $\boldsymbol{V}_{h,\mathrm{ort}}$ is a finite element function and therefore *numerically computable*. We refer to this particular choice for the space of $\tilde{\boldsymbol{U}}$, motivated by the election (35) and the approximation (36), as the *space of orthogonal sub-scales*.

We still have to approximate $\tilde{U}_{\mathrm{ske}}$ in (30) and solve for $\tilde{\boldsymbol{U}}$ in (30). For that we follow the same steps as in the algebraic sub-grid scale method. First we assume that $\tilde{U}_{\mathrm{ske}} \approx \boldsymbol{0}$ and therefore $\tilde{\boldsymbol{U}}$ can be written formally as

$$\tilde{\boldsymbol{U}} = \mathscr{L}_0^{-1}[\boldsymbol{F} - \mathscr{L}(\boldsymbol{U}_h)] + \tilde{\boldsymbol{V}}_{h,\mathrm{ort}} \in \mathscr{W}_h^{\perp},$$

where $\mathscr{L}_0^{-1}$ is the inverse of $\mathscr{L}$ with homogeneous Dirichlet conditions and $\tilde{\boldsymbol{V}}_{h,\mathrm{ort}} = \mathscr{L}_0^{-1}\boldsymbol{V}_{h,\mathrm{ort}}$.

From (32), which is also the stabilized equation in this case, it is seen that only the component of $\tilde{\boldsymbol{U}}$ on $\mathscr{L}(\mathscr{W}_h)$ is needed. As for the algebraic sub-grid scale method, this suggests to approximate $\tilde{\boldsymbol{U}}$ as

$$\tilde{\boldsymbol{U}} = \boldsymbol{\tau}[\boldsymbol{F} - \mathscr{L}(\boldsymbol{U}_h)] + \tilde{\boldsymbol{V}}_{h,\mathrm{ort}} \in \mathscr{W}_h^{\perp}, \tag{39}$$

that is, to take $\mathscr{L}_0^{-1} \approx \boldsymbol{\tau}$.

Analogous to Section 3, let $P_{h,12}$ be the L^2 orthogonal projection onto $\mathscr{W}_h$, with $P_{h,1}$ the projection onto $\mathscr{W}_{h,0}$ and $P_{h,2}$ the projection onto $\mathscr{W}_{h,0}^{\perp} \cap \mathscr{W}_h$. Let also $P_{h,3}$ be the orthogonal projection onto $\mathscr{W}_h^{\perp}$. Imposing that $\tilde{\boldsymbol{U}}$ must belong to $\mathscr{W}_h^{\perp}$, it follows from (39) that

$$\tilde{\boldsymbol{V}}_{h,\mathrm{ort}} = -P_{h,12}\{\boldsymbol{\tau}[\boldsymbol{F} - \mathscr{L}(\boldsymbol{U}_h)]\},$$

that is,

$$\tilde{\boldsymbol{U}} = P_{h,3}\{\boldsymbol{\tau}[\boldsymbol{F} - \mathscr{L}(\boldsymbol{U}_h)]\}. \tag{40}$$

This is the expression that has to be inserted now in (32).

4.2. Application to the Stokes problem

The objective now is to show that the previous method is closely related to the stabilization based on the projection of the pressure gradient presented in Section 2. Assume that:

- $\boldsymbol{\tau} = \mathrm{diag}(\tau_1, \tau_1, 0)$ (in 2D) is the same for all the elements (quasi-uniform meshes).
- $P_{h,3}\boldsymbol{F} = \boldsymbol{0}$ (the force vector belongs to the finite element space $\mathscr{W}_h$).
- Linear or bilinear elements are used, with $\Delta \boldsymbol{U}_h = \Delta \boldsymbol{V}_h = \boldsymbol{0}$ within each element.

Under these conditions, the resulting stabilizing term is:

$$\int_{\Omega'} \mathscr{L}^*(\boldsymbol{V}_h)^{\mathrm{t}} \tilde{\boldsymbol{U}}\, \mathrm{d}\Omega = \int_{\Omega'} \mathscr{L}^*(\boldsymbol{V}_h)^{\mathrm{t}} P_{h,3}\{\boldsymbol{\tau}[\boldsymbol{F} - \mathscr{L}(\boldsymbol{U}_h)]\}\, \mathrm{d}\Omega = \int_{\Omega'} \tau_1 \nabla q_h \cdot P_{h,3}(\nabla p_h)\, \mathrm{d}\Omega$$
$$= \int_{\Omega'} \tau_1 \nabla q_h \cdot [\nabla p_h - P_{h,12}(\nabla p_h)]\, \mathrm{d}\Omega.$$

Calling $\boldsymbol{\xi}_h = P_{h,12}(\nabla p_h)$ and using the fact that

$$(\nabla p_h, \boldsymbol{\eta}_h) = (\boldsymbol{\xi}_h, \boldsymbol{\eta}_h) \quad \forall \boldsymbol{\eta}_h \in \mathscr{V}_h,$$

the bilinear form associated to the problem is

$$B(\boldsymbol{u}_h, p_h, \boldsymbol{\xi}_h; \boldsymbol{v}_h, q_h, \boldsymbol{\eta}_h) = a(\boldsymbol{u}_h, \boldsymbol{v}_h) - b(p_h, \boldsymbol{v}_h) + \tau_1(\nabla p_h, \nabla q_h) - \tau_1(\boldsymbol{\xi}_h, \nabla q_h) + b(q_h, \boldsymbol{u}_h) - \tau_1(\nabla p_h, \boldsymbol{\eta}_h)$$
$$+ \tau_1(\boldsymbol{\xi}_h, \boldsymbol{\eta}_h).$$

The problem can be formulated as: find $(\boldsymbol{u}_h, p_h, \boldsymbol{\xi}_h) \in \mathscr{V}_{h,0} \times \mathscr{Q}_h \times \mathscr{V}_h$ such that

$$B(\boldsymbol{u}_h, p_h, \boldsymbol{\xi}_h; \boldsymbol{v}_h, q_h, \boldsymbol{\eta}_h) = (\boldsymbol{f}, \boldsymbol{v}_h) \quad \forall (\boldsymbol{v}_h, q_h, \boldsymbol{\eta}_h) \in \mathscr{V}_{h,0} \times \mathscr{Q}_h \times \mathscr{V}_h,$$

which is *exactly* the stabilized Stokes problem using the pressure gradient projection given by (14)–(16) identifying $\alpha \equiv \tau_1$.

5. Stabilization of convection

In the previous section, it has been shown how to apply the idea of the stabilization with orthogonal subscales to the Stokes problem. However, the same concept can be applied to other problems as well, and in this section it is shown how to apply it to stabilize convection. We start with the simple convection–diffusion–reaction equation and then move to the Navier–Stokes equations as an example of problem involving both incompressibility and convection.

5.1. Convection–diffusion–reaction equation

Let us consider now the problem of finding a scalar function u such that:

$$\begin{aligned} &\mathscr{L}(u) := -k\,\Delta u + \boldsymbol{a} \cdot \nabla u + s u = f \quad \text{in } \Omega, \\ &u = 0 \quad \text{on } \partial\Omega, \end{aligned} \tag{41}$$

with $\boldsymbol{a}$ a bounded and smooth solenoidal field ($\nabla \cdot \boldsymbol{a} = 0$), and $s \geqslant 0$, $k > 0$, the constants.

The bilinear and linear forms associated to the problem are now

$$B(u, v) = k(\nabla u, \nabla v) + (\boldsymbol{a} \cdot \nabla u, v) + s(u, v),$$
$$L(v) = (f, v).$$

Consider finite element spaces $\mathscr{V}_h \subset H^1(\Omega)$, $\mathscr{V}_{h,0} \subset H^1_0(\Omega)$. To introduce the method, assume that:

- Linear elements are used.
- τ is the same for all the elements.
- $f \in \mathscr{V}_h$.

Under these conditions, the stabilizing term coming from the orthogonal sub-scales is

$$\begin{aligned}
&\int_{\Omega'} \mathscr{L}^*(v_h) P_{h,3}\{\tau[f - \mathscr{L}(u_h)]\}\,\mathrm{d}\Omega \\
&\quad = \tau \int_{\Omega'} (-k\Delta v_h - \boldsymbol{a}\cdot\nabla v_h + s v_h) P_{h,3}(f + k\Delta u_h - \boldsymbol{a}\cdot\nabla u_h - s u_h)\,\mathrm{d}\Omega \\
&\quad = \tau \int_{\Omega'} (\boldsymbol{a}\cdot\nabla v_h) P_{h,3}(\boldsymbol{a}\cdot\nabla u_h)\,\mathrm{d}\Omega \\
&\quad \equiv \tau(\boldsymbol{a}\cdot\nabla v_h, P_{h,3}(\boldsymbol{a}\cdot\nabla u_h)),
\end{aligned} \tag{42}$$

and thus the bilinear form associated to the stabilized problem is

$$B_{\mathrm{stab}}(u_h, v_h) = B(u_h, v_h) + \tau(\boldsymbol{a}\cdot\nabla v_h, P_{h,3}(\boldsymbol{a}\cdot\nabla u_h)), \tag{43}$$

which can be written alternatively as

$$B_{\mathrm{stab}}(u_h, \xi_h; v_h, \eta_h) = B(u_h, v_h) + \tau(\boldsymbol{a}\cdot\nabla v_h - \eta_h, \boldsymbol{a}\cdot\nabla u_h - \xi_h), \tag{44}$$

with B_{stab} now defined on $(\mathscr{V}_{h,0}\times\mathscr{V}_h)^2$. Clearly, this form can be also extended to $(H_0^1(\Omega)\times L^2(\Omega))^2$ for the continuous problem. In the convergence analysis presented below, we use (44) to define the problem, since it highlights in which sense the method is *consistent*.

Remark 4. Even though (43) has been motivated by the use of orthogonal sub-scales and making use of certain assumptions, *it constitutes a stabilized bilinear form that can be used in any case*, since the resulting problem will be consistent. To avoid technicalities, we shall restrict ourselves to quasi-uniform meshes, but this condition can also be relaxed by considering the stabilization parameter τ defined element-wise.

The stabilized problem is then: find $(u_h, \xi_h)\in\mathscr{V}_{h,0}\times\mathscr{V}_h$ such that

$$B_{\mathrm{stab}}(u_h, \xi_h; v_h, \eta_h) = L(v_h) \quad \forall (v_h, \eta_h)\in\mathscr{V}_{h,0}\times\mathscr{V}_h.$$

To prove convergence, we need a rather technical condition, which is analogous to (20) but adapted to the present problem. The version of this condition employed below is: there exists a constant $C>0$ such that

$$\|\boldsymbol{a}\cdot\nabla v_h\| \leqslant C\|P_{h,13}(\boldsymbol{a}\cdot\nabla v_h)\| \quad \forall v_h\in\mathscr{V}_{h,0}. \tag{45}$$

Using exactly the same analysis as in [1], it can be shown that this condition holds under a mild regularity condition on the finite element mesh (all the possible macroelements have a vertex interior to Ω) and also on the velocity field $\boldsymbol{a}$.

The final ingredient needed is the following inverse estimate:

$$\|\nabla v_h\| \leqslant \frac{C_{\mathrm{inv}}}{h}\|v_h\|, \tag{46}$$

which holds for any finite element function $v_h\in\mathscr{V}_h$ if we consider quasi-uniform finite element partitions of diameter h.

The proof of the following convergence result explains the stabilization mechanism introduced by (42):

Theorem 2. *Suppose that the family of finite element partitions is such that* (45) *and* (46) *hold and the elements are of order p. Let*

$$\tau = \left(c_1\frac{k}{h^2} + c_2\frac{|\boldsymbol{a}|_\infty}{h} + c_3 s\right)^{-1}, \tag{47}$$

where c_1, c_2 and c_3 *are positive algorithmic constants and* $|\boldsymbol{a}|_\infty$ *is the maximum of the Euclidean norm of* $\boldsymbol{a}$. *Then, if the solution u to the continuous problem* (41) *belongs to* $H^{p+1}(\Omega)$, *the solution* u_h *to the discrete problem verifies the error estimate*

$$|||u-u_h||| \leqslant C\left(k^{1/2}h^p + s^{1/2}h^{p+1} + |\boldsymbol{a}|_\infty^{1/2}h^{p+1/2}\right), \tag{48}$$

where C is a constant independent of h and $|||\cdot|||$ is defined as

$$|||u||| := k^{1/2}\|\nabla u\| + s^{1/2}\|u\| + \tau^{1/2}\|\boldsymbol{a}\cdot\nabla u\|, \quad u \in H^1(\Omega).$$

Proof. From the definition (44) of B_{stab} the following stability estimate is found:

$$B_{\text{stab}}(v,\eta;v,\eta) = k\|\nabla v\|^2 + s\|v\|^2 + \tau\|\boldsymbol{a}\cdot\nabla v - \eta\|^2 \quad \forall (v,\eta) \in H_0^1(\Omega)\times L^2(\Omega). \tag{49}$$

On the other hand, the exact solution u satisfies

$$B_{\text{stab}}(u, \boldsymbol{a}\cdot\nabla u; v_h, \eta_h) = (f, v_h) \quad \forall (v_h,\eta_h) \in \mathscr{V}_{h,0}\times\mathscr{V}_h,$$

from where the following consistency condition follows:

$$B_{\text{stab}}(u-u_h, \boldsymbol{a}\cdot\nabla u - \xi_h; v_h, \eta_h) = 0 \quad \forall (v_h,\eta_h) \in \mathscr{V}_{h,0}\times\mathscr{V}_h. \tag{50}$$

From (49) applied to $(v,\eta) = (u-u_h, \boldsymbol{a}\cdot\nabla u - \xi_h)$ and from (50) we have that

$$\begin{aligned} &k\|\nabla u - \nabla u_h\|^2 + s\|u-u_h\|^2 + \tau\|\boldsymbol{a}\cdot\nabla u_h - \xi_h\|^2 \\ &\quad = B_{\text{stab}}(u-u_h, \boldsymbol{a}\cdot\nabla u - \xi_h; u-u_h, \boldsymbol{a}\cdot\nabla u - \xi_h) \\ &\quad = B_{\text{stab}}(u-u_h, \boldsymbol{a}\cdot\nabla u - \xi_h; u-v_h, \boldsymbol{a}\cdot\nabla u - \eta_h) \quad \forall (v_h,\eta_h) \in \mathscr{V}_{h,0}\times\mathscr{V}_h. \end{aligned} \tag{51}$$

Let $\hat{u}_h$ be the finite element interpolant of u in $\mathscr{V}_{h,0}$ and $\hat{\xi}_h$ the finite element interpolant of $\boldsymbol{a}\cdot\nabla u$ in $\mathscr{V}_h$. Using (51) with $(v_h,\eta_h) = (\hat{u}_h, \hat{\xi}_h)$ and Schwartz's inequality we have that

$$\begin{aligned} &k\|\nabla u - \nabla u_h\|^2 + s\|u-u_h\|^2 + \tau\|\boldsymbol{a}\cdot\nabla u_h - \xi_h\|^2 \\ &\quad \leqslant k\|\nabla u - \nabla u_h\|\|\nabla u - \nabla\hat{u}_h\| + s\|u-u_h\|\|u-\hat{u}_h\| + \|\boldsymbol{a}\cdot\nabla u - \boldsymbol{a}\cdot\nabla u_h\|\|u-\hat{u}_h\| \\ &\quad + \tau\|\boldsymbol{a}\cdot\nabla u_h - \xi_h\|\|\boldsymbol{a}\cdot\nabla\hat{u}_h - \hat{\xi}_h\|. \end{aligned} \tag{52}$$

Let us introduce the notation

$$\begin{aligned} &E_0(u) := \|u-u_h\|, \quad I_0(u) := \|u-\hat{u}_h\|, \\ &E_1(u) := \|\nabla u - \nabla u_h\|, \quad I_1(u) := \|\nabla u - \nabla\hat{u}_h\|, \\ &E_a(u) := \|\boldsymbol{a}\cdot\nabla u - \boldsymbol{a}\cdot\nabla u_h\|, \quad I_a(u) := \|\boldsymbol{a}\cdot\nabla u - \boldsymbol{a}\cdot\nabla\hat{u}_h\|, \\ &I_0(\boldsymbol{a}\cdot\nabla u) := \|\boldsymbol{a}\cdot\nabla u - \hat{\xi}_h\|, \quad G := \|\boldsymbol{a}\cdot\nabla u_h - \xi_h\|. \end{aligned}$$

The finite element errors have been denoted by E and the interpolation errors by I. Noting that

$$\|\boldsymbol{a}\cdot\nabla\hat{u}_h - \hat{\xi}_h\| \leqslant \|\boldsymbol{a}\cdot\nabla\hat{u}_h - \boldsymbol{a}\cdot\nabla u\| + \|\boldsymbol{a}\cdot\nabla u - \hat{\xi}_h\| = I_a(u) + I_0(\boldsymbol{a}\cdot\nabla u),$$

this notation allows us to write (52) as

$$kE_1^2(u) + sE_0^2(u) + \tau G^2 \leqslant kE_1(u)I_1(u) + sE_0(u)I_0(u) + E_a(u)I_0(u) + \tau G I_a(u) + \tau G I_0(\boldsymbol{a}\cdot\nabla u). \tag{53}$$

Note the presence of the finite element error of the streamline derivative $E_a(u)$ in the right-hand side (RHS) of (53), which is absent in the left-hand side. When $\tau = 0$ there is no way to control this term. However, we shall see that the presence of τG^2 is enough to have control over $E_a(u)$.

Using the triangle inequality and the stability condition (45) we obtain

$$\begin{aligned}
E_a(u) &\leqslant \|\boldsymbol{a}\cdot\nabla u - P_{h,12}(\boldsymbol{a}\cdot\nabla\hat{u}_h)\| + \|P_{h,12}(\boldsymbol{a}\cdot\nabla\hat{u}_h) - \boldsymbol{a}\cdot\nabla u_h\| \\
&\leqslant \|\boldsymbol{a}\cdot\nabla u - P_{h,12}(\boldsymbol{a}\cdot\nabla\hat{u}_h)\| + \|P_{h,1}(\boldsymbol{a}\cdot\nabla\hat{u}_h) - P_{h,1}(\boldsymbol{a}\cdot\nabla u_h)\| \\
&\quad + \|P_{h,2}(\boldsymbol{a}\cdot\nabla\hat{u}_h) - P_{h,2}(\boldsymbol{a}\cdot\nabla u_h)\| + \|P_{h,3}(\boldsymbol{a}\cdot\nabla u_h)\| \\
&\leqslant C\Big\{\|\boldsymbol{a}\cdot\nabla u - P_{h,12}(\boldsymbol{a}\cdot\nabla\hat{u}_h)\| + \|P_{h,1}(\boldsymbol{a}\cdot\nabla\hat{u}_h) - P_{h,1}(\boldsymbol{a}\cdot\nabla u_h)\| + \|\boldsymbol{a}\cdot\nabla\hat{u}_h - \boldsymbol{a}\cdot\nabla u\| \\
&\quad + \|\boldsymbol{a}\cdot\nabla u - P_{h,12}(\boldsymbol{a}\cdot\nabla\hat{u}_h)\| + \|P_{h,3}(\boldsymbol{a}\cdot\nabla u_h)\|\Big\} \\
&\leqslant C\Big\{\|\boldsymbol{a}\cdot\nabla u - P_{h,12}(\boldsymbol{a}\cdot\nabla\hat{u}_h)\| + \|P_{h,1}(\boldsymbol{a}\cdot\nabla\hat{u}_h) - P_{h,1}(\boldsymbol{a}\cdot\nabla u_h)\| + I_a(u) + G\Big\}. \qquad (54)
\end{aligned}$$

We have to bound now the first two terms in the RHS of this inequality. Observe first that

$$\|\boldsymbol{a}\cdot\nabla u - P_{h,12}(\boldsymbol{a}\cdot\nabla\hat{u}_h)\| \leqslant \|\boldsymbol{a}\cdot\nabla u - P_{h,12}(\boldsymbol{a}\cdot\nabla u)\| + \|P_{h,12}(\boldsymbol{a}\cdot\nabla u) - P_{h,12}(\boldsymbol{a}\cdot\nabla\hat{u}_h)\|. \qquad (55)$$

Since $P_{h,12}(\boldsymbol{a}\cdot\nabla u)$ is the projection of $\boldsymbol{a}\cdot\nabla u$ onto $\mathscr{V}_h$ we have

$$\begin{aligned}
\|\boldsymbol{a}\cdot\nabla u - P_{h,12}(\boldsymbol{a}\cdot\nabla u)\|^2 &= (\boldsymbol{a}\cdot\nabla u - P_{h,12}(\boldsymbol{a}\cdot\nabla u), \boldsymbol{a}\cdot\nabla u - P_{h,12}(\boldsymbol{a}\cdot\nabla u) + P_{h,12}(\boldsymbol{a}\cdot\nabla u) - \hat{\xi}_h) \\
&\leqslant \|\boldsymbol{a}\cdot\nabla u - P_{h,12}(\boldsymbol{a}\cdot\nabla u)\|\|\boldsymbol{a}\cdot\nabla u - \hat{\xi}_h\|,
\end{aligned}$$

which together with the fact that the norm of projection operators is $\leqslant 1$ applied to (55) implies

$$\|\boldsymbol{a}\cdot\nabla u - P_{h,12}(\boldsymbol{a}\cdot\nabla\hat{u}_h)\| \leqslant I_0(\boldsymbol{a}\cdot\nabla u) + I_a(u). \qquad (56)$$

Let us deal now with the second term in the RHS of (54), which can be split as

$$\begin{aligned}
\|P_{h,1}(\boldsymbol{a}\cdot\nabla u_h) - P_{h,1}(\boldsymbol{a}\cdot\nabla\hat{u}_h)\|^2 &= (\boldsymbol{a}\cdot\nabla u_h - \boldsymbol{a}\cdot\nabla u, P_{h,1}(\boldsymbol{a}\cdot\nabla u_h) - P_{h,1}(\boldsymbol{a}\cdot\nabla\hat{u}_h)) \\
&\quad + (\boldsymbol{a}\cdot\nabla u - \boldsymbol{a}\cdot\nabla\hat{u}_h, P_{h,1}(\boldsymbol{a}\cdot\nabla u_h) - P_{h,1}(\boldsymbol{a}\cdot\nabla\hat{u}_h)). \qquad (57)
\end{aligned}$$

The key point to bound the first term is to use the consistency condition (50) taking $(v_h,\eta_h) = (P_{h,1}(\boldsymbol{a}\cdot\nabla\hat{u}_h) - P_{h,1}(\boldsymbol{a}\cdot\nabla u_h), 0)$. Here also the inverse estimate (46) and the expression (47) of τ need to be used. This yields

$$\begin{aligned}
&(\boldsymbol{a}\cdot\nabla u_h - \boldsymbol{a}\cdot\nabla u, P_{h,1}(\boldsymbol{a}\cdot\nabla u_h) - P_{h,1}(\boldsymbol{a}\cdot\nabla\hat{u}_h)) \\
&\quad = k(\nabla u - \nabla u_h, \nabla P_{h,1}(\boldsymbol{a}\cdot\nabla u_h) - \nabla P_{h,1}(\boldsymbol{a}\cdot\nabla\hat{u}_h)) + s(u - u_h, P_{h,1}(\boldsymbol{a}\cdot\nabla u_h) - P_{h,1}(\boldsymbol{a}\cdot\nabla\hat{u}_h)) \\
&\qquad + \tau(\xi_h - \boldsymbol{a}\cdot\nabla u_h, \boldsymbol{a}\cdot\nabla P_{h,1}(\boldsymbol{a}\cdot\nabla u_h) - \boldsymbol{a}\cdot\nabla P_{h,1}(\boldsymbol{a}\cdot\nabla\hat{u}_h)) \\
&\quad \leqslant k^{1/2}E_1(u)\tau^{-1/2}\|P_{h,1}(\boldsymbol{a}\cdot\nabla u_h) - P_{h,1}(\boldsymbol{a}\cdot\nabla\hat{u}_h)\| + s^{1/2}E_0(u)\tau^{-1/2}\|P_{h,1}(\boldsymbol{a}\cdot\nabla u_h) - P_{h,1}(\boldsymbol{a}\cdot\nabla\hat{u}_h)\| \\
&\qquad + G\|P_{h,1}(\boldsymbol{a}\cdot\nabla u_h) - P_{h,1}(\boldsymbol{a}\cdot\nabla\hat{u}_h)\|. \qquad (58)
\end{aligned}$$

The second term in (57) is easy to bound

$$(\boldsymbol{a}\cdot\nabla u - \boldsymbol{a}\cdot\nabla\hat{u}_h, P_{h,1}(\boldsymbol{a}\cdot\nabla u_h) - P_{h,1}(\boldsymbol{a}\cdot\nabla\hat{u}_h)) \leqslant I_a(u)\|P_{h,1}(\boldsymbol{a}\cdot\nabla u_h) - P_{h,1}(\boldsymbol{a}\cdot\nabla\hat{u}_h)\|.$$

Using this and (58) it follows from (57) that

$$\|P_{h,1}(\boldsymbol{a}\cdot\nabla u_h) - P_{h,1}(\boldsymbol{a}\cdot\nabla\hat{u}_h)\| \leqslant k^{1/2}E_1(u)\tau^{-1/2} + s^{1/2}E_0(u)\tau^{-1/2} + G + I_a(u).$$

Using this inequality and (56) in (54) yields

$$\tau^{1/2}E_a(u) \leqslant C\big\{k^{1/2}E_1(u) + s^{1/2}E_0(u) + \tau^{1/2}[G + I_a(u) + I_0(\boldsymbol{a}\cdot\nabla u)]\big\}. \qquad (59)$$

Using this inequality in (53) yields

$$kE_1^2(u) + sE_0^2(u) + \tau G^2 \leqslant C\big[\big(k^{1/2}E_1(u) + s^{1/2}E_0(u) + \tau^{1/2}G\big)\psi_0(h) + \psi_1(h)\big], \qquad (60)$$

where

$$\psi_0(h) := \tau^{-1/2}[hI_1(u) + I_0(u)] + \tau^{1/2}[I_a(u) + I_0(\boldsymbol{a}\cdot\nabla u)]$$

$$\psi_1(h) := I_0(u)[I_a(u) + I_0(\boldsymbol{a}\cdot\nabla u)].$$

Since

$$\psi_0(h) \leqslant \frac{1}{2}\tau^{-1}I_0^2(u) + \frac{1}{2}\tau[I_a(u) + I_0(\boldsymbol{a}\cdot\nabla u)]^2,$$

from (60) we have that

$$k^{1/2}E_1(u) + s^{1/2}E_0(u) + \tau^{1/2}G \leqslant C\psi_0(h).$$

The theorem follows from this, (59) and the standard approximation properties of the interpolation functions. □

Remark 5. The convergence estimate (48) is the same as for the SUPG or the GLS methods [15], even in the presence of reaction [16]. This error estimate is globally optimal. However, the local behavior of all these methods can be quite different. This is further discussed in Section 6.1.

Remark 6. The stabilizing term (42) does not account for dominant reactive terms s, since the orthogonal projection of su_h is obviously zero. Therefore, the localized oscillations near boundaries appearing in these cases are not removed by the use of the stabilization with orthogonal sub-scales (see [13] for further discussion in a more general problem). The reason for this can be traced back to the fact that (36) tacitly implies that we seek the finite element solution as the L^2 projection of the continuous solution u onto the finite element space. These projections allow for boundary oscillations.

5.2. Navier–Stokes equations

The most important problem that combines convection and incompressibility is undoubtedly the incompressible Navier–Stokes equations. The problem we consider here is

$$\boldsymbol{a}\cdot\nabla\boldsymbol{u} - \nu\Delta\boldsymbol{u} + \nabla p = \boldsymbol{f} \quad \text{in } \Omega, \tag{61}$$

$$\nabla\cdot\boldsymbol{u} = 0 \quad \text{in } \Omega, \tag{62}$$

where $\boldsymbol{a}$ is either given for the linearized Navier–Stokes equations (Oseen equations) or $\boldsymbol{a} = \boldsymbol{u}$ for the original nonlinear problem.

The extension of the orthogonal sub-scale stabilization to problem (61) and (62) is straightforward once the convection–diffusion and the Stokes problems have been dealt with.

The adjoint of the linearized Navier–Stokes operator applied to the finite element test functions is now

$$\mathscr{L}^*(\boldsymbol{V}_h) = \begin{bmatrix} -\nabla\cdot(\boldsymbol{a}\otimes\boldsymbol{v}_h) - \nu\Delta\boldsymbol{v}_h - \nabla q_h \\ -\nabla\cdot\boldsymbol{v}_h \end{bmatrix}.$$

Assuming $\boldsymbol{a}$ to be divergence free, $\boldsymbol{f}$ in the finite element space, that linear interpolations are used and taking the matrix of stabilization parameters as in (34), the stabilizing term to be added to the Galerkin bilinear form of the problem is

$$\int_{\Omega'} \mathscr{L}^*(\boldsymbol{V}_h)^{\mathrm{t}} P_{h,3}\{\boldsymbol{\tau}[\boldsymbol{F} - \mathscr{L}(\boldsymbol{U}_h)]\}\,\mathrm{d}\Omega = \int_{\Omega'} \tau_1(\boldsymbol{a}\cdot\nabla\boldsymbol{v}_h + \nabla q_h)\cdot P_{h,3}(\boldsymbol{a}\cdot\nabla\boldsymbol{u}_h + \nabla p_h)\,\mathrm{d}\Omega + \int_{\Omega'} \tau_2(\nabla\cdot\boldsymbol{v}_h)P_{h,3}(\nabla\cdot\boldsymbol{u}_h)\,\mathrm{d}\Omega. \tag{63}$$

The parameters τ_1 and τ_2 proposed are the same as in [13]

$$\tau_1 = \left(\frac{c_1 \nu}{h^2} + c_2 \frac{|\boldsymbol{a}|_\infty}{h} \right)^{-1}, \quad \tau_2 = c_3 \frac{h^2}{\tau_1}.$$

In the numerical examples, we have taken the algorithmic constants as $c_1 = 4$, $c_2 = 2$ and $c_3 = 1$. Likewise, (63) has been employed even for quadratic interpolations and general vectors of body forces, since the resulting method is consistent (an equation analogous to (50) holds in this case).

Remark 7. Even though the stabilizing term (63) is the one that results in a natural way from the sub-grid scale approach using orthogonal sub-scales, it is also possible to use a sort of 'term-by-term' stabilization, which would lead to the stabilizing term

$$\int_{\Omega'} \tau_1 (\boldsymbol{a} \cdot \nabla \boldsymbol{v}_h) \cdot P_{h,3}(\boldsymbol{a} \cdot \nabla \boldsymbol{u}_h) \, \mathrm{d}\Omega + \int_{\Omega'} \tau_1' (\nabla q_h) \cdot P_{h,3}(\nabla p_h) \, \mathrm{d}\Omega + \int_{\Omega'} \tau_2 (\nabla \cdot \boldsymbol{v}_h) P_{h,3}(\nabla \cdot \boldsymbol{u}_h) \, \mathrm{d}\Omega, \tag{64}$$

instead of (63). The parameters τ_1 and τ_1' could even be taken different. Dropping the orthogonal projection $P_{h,3}$, the method reduces to that analyzed in [17], which has a consistency error that makes it only applicable with P_1 elements. The possibility of using (64) needs to be further explored.

6. Numerical experiments

In this section, some tests are conducted to show the numerical performance of the orthogonal sub-scale stabilization, hereafter referred to as OSS. It is compared with the algebraic sub-grid scale method (ASGS),

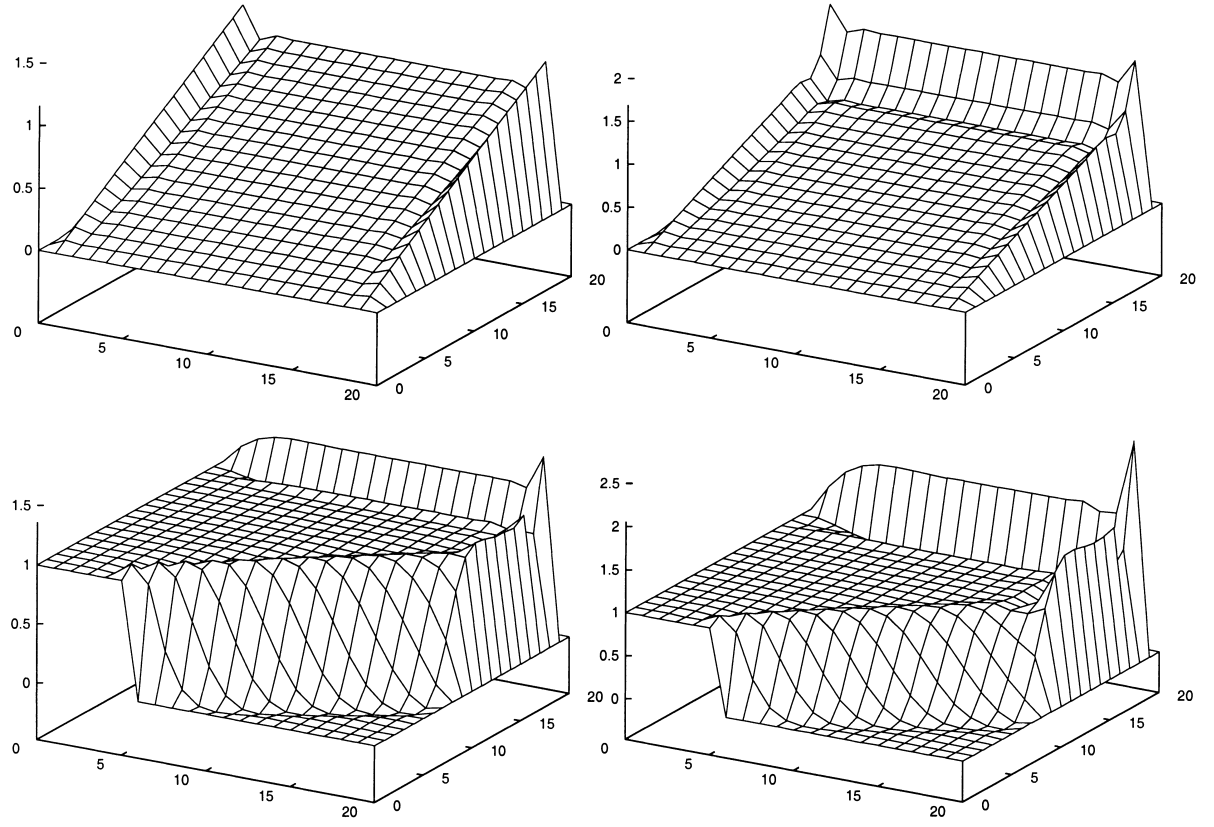

Fig. 1. Elevation plots of the unknown for Example 1. Left: ASGS method; right: OSS method. Top: case 1; bottom: case 2.

as described in Section 3.2.2. Therefore, the methods to be compared both consist in introducing the stabilizing term (32), with

$$\begin{aligned} &\tilde{\boldsymbol{U}} = -\boldsymbol{\tau}[\mathscr{L}(\boldsymbol{U}_h) - \boldsymbol{F}] \quad \text{for the ASGS method,} \\ &\tilde{\boldsymbol{U}} = -P_{h,3}\{\boldsymbol{\tau}\mathscr{L}(\boldsymbol{U}_h)\} = -\{\boldsymbol{\tau}\mathscr{L}(\boldsymbol{U}_h) - P_{h,12}[\boldsymbol{\tau}\mathscr{L}(\boldsymbol{U}_h)]\} \quad \text{for the OSS method.} \end{aligned} \tag{65}$$

In both cases, the matrix of stabilization parameters is taken as indicated in (47) for the scalar convection–diffusion equation and as described in the previous section for the Stokes and Navier–Stokes problems.

Concerning the OSS method, it has been implemented iteratively, evaluating the projection $P_{h,12}[\boldsymbol{\tau}\mathscr{L}(\boldsymbol{U}_h)]$ at iteration $i-1$ when the unknown at iteration i is sought. In all the cases, the convergence tolerance has been taken as the $10^{-3}\%$ of the initial residual. The computational domain for all the examples is the unit square $\Omega = (0,1) \times (0,1)$.

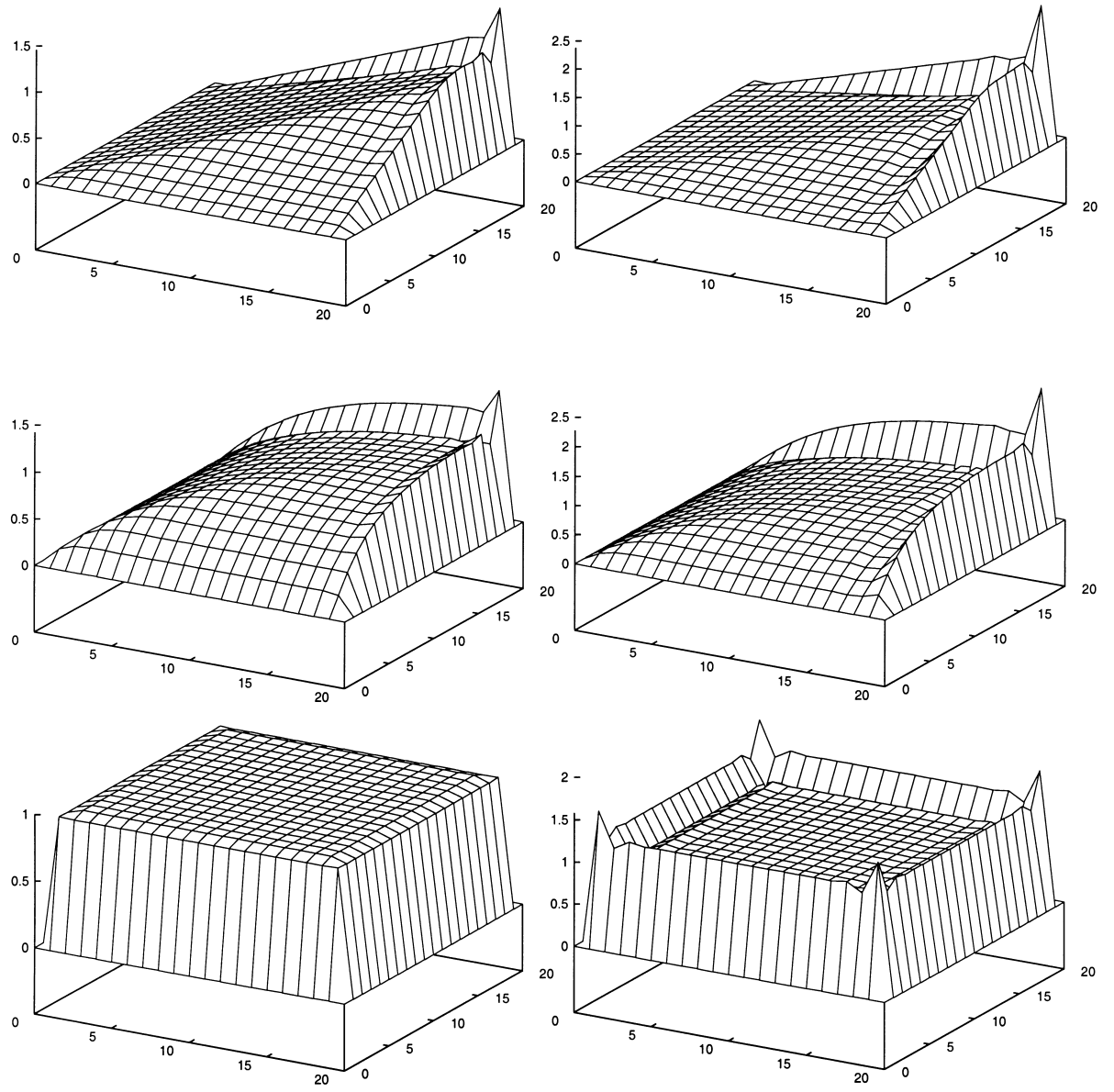

Fig. 2. Elevation plots of the unknown for Example 1. Left: ASGS method; right: OSS method. Top: case 3; middle: case 4; bottom: case 5.

6.1. Convection–diffusion–reaction tests

In this first series of tests, the convection–diffusion–reaction equation (41) is numerically solved. In all the cases, the diffusion coefficient is taken as $k = 10^{-4}$, and different combinations of the rest of coefficients are considered. The finite element mesh employed consists of 20×20 Q_1 elements. If $\bar{u}$ denotes the boundary condition for u, the cases considered are:

1. $f = 1$, $s = 0$, $\boldsymbol{a} = (0,1)$, $\bar{u} = 0$
2. $f = 0$, $s = 0$, $\boldsymbol{a} = (3,2)$, $\bar{u} = 1$ on $\Gamma_1 = [0, 0.25] \times \{0\}$, $\bar{u} = 0$ on $\partial\Omega \setminus \Gamma_1$.
3. $f = 3$, $s = 0$, $\boldsymbol{a} = (3,2)$, $\bar{u} = 0$.
4. $f = 10$, $s = 10$, $\boldsymbol{a} = (3,2)$, $\bar{u} = 0$.
5. $f = 10$, $s = 10$, $\boldsymbol{a} = (0,0)$, $\bar{u} = 0$.

The elevation plots of the numerical solution in the first two cases are shown in Fig. 1 (in this and the following figure the coordinates are measured in grid units). Both the ASGS and the OSS yield very similar solutions in the interior of the computational domain, but the former yields smaller overshoots near the boundaries. This, however, depends on the angle formed by the velocity and the boundary. In particular, in the first case the overshoots near the boundaries parallel to $\boldsymbol{a}$ are almost the same using both methods.

The next three cases are intended to analyze the effect of s in the numerical solution. The elevation plots are shown in Fig. 2. The same behavior as before is consistently observed now. In particular, when $\boldsymbol{a} = (0,0)$ (case 5) the OSS does not act, and the same localized oscillations as in the Galerkin method remain.

To better observe the difference between the solutions obtained using the ASGS and the OSS methods, they are plotted along a mid-section in Fig. 3 (corresponding to Fig. 1) and Fig. 4 (corresponding to Fig. 2). These figures clearly indicate that the ASGS and the OSS formulations only yield different results near

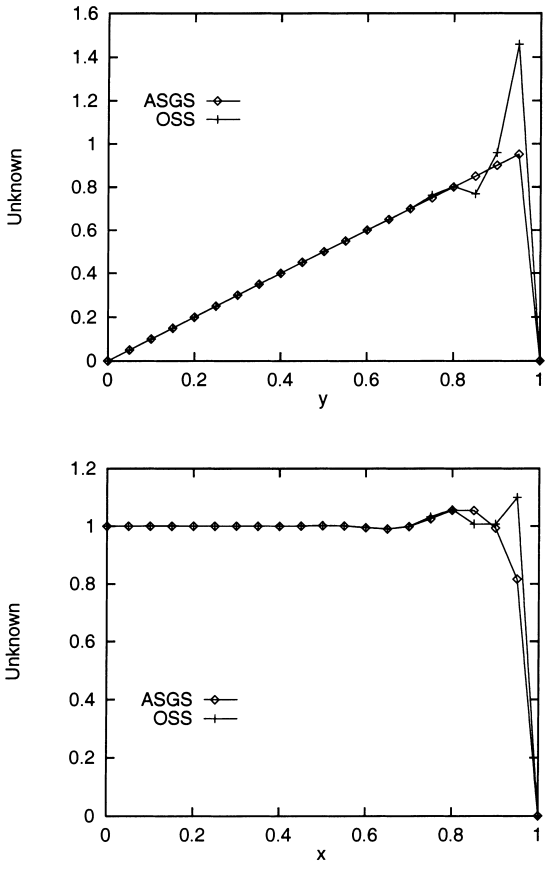

Fig. 3. Sections of the unknown for Example 1. Left: ASGS method; right: OSS method. Top: case 1; bottom: case 2.

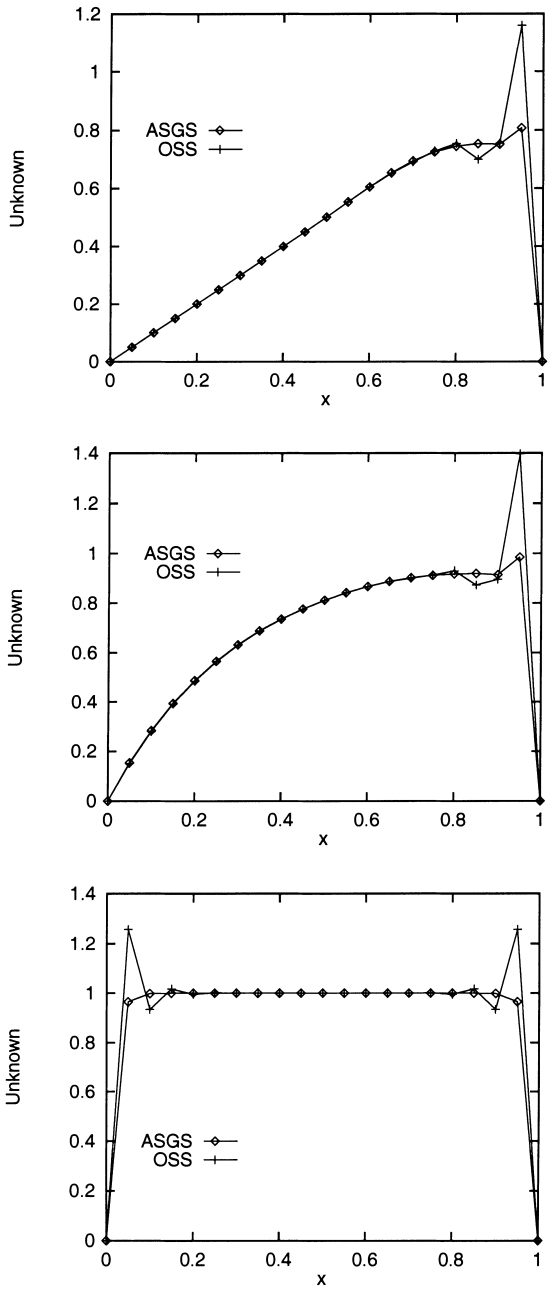

Fig. 4. Sections of the unknown for Example 1. Left: ASGS method; right: OSS method. Top: case 3; middle: case 4; bottom: case 5.

layers. Since none of these methods is monotone, both are expected to yield oscillations, being stronger those of the OSS method. However, this needs not to be considered as a bad result for this formulation. Firstly, because comparisons should be made combining the ASGS and the OSS methods with a discontinuity-capturing mechanism, and secondly because in some cases it might be convenient to use methods able to capture steep slopes near boundaries, as the OSS method does.

6.2. Stokes flow in a cavity

Whereas in the previous example it has been shown that the ASGS yields less overshoots near boundaries, the accuracy when $\boldsymbol{a}$ is parallel to the boundary (or zero) is higher using the OSS method. This

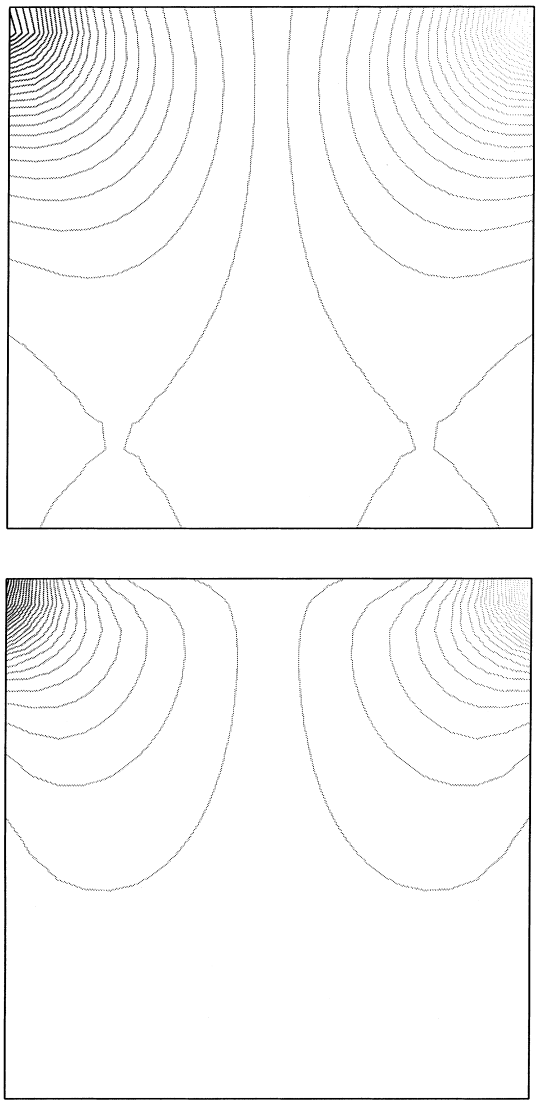

Fig. 5. Pressure contours for the Stokes problem with $\boldsymbol{a} = (0,0)$. Top: ASGS; bottom: OSS.

point was already discussed in [1] for the Stokes problem. Here, a very simple and popular example is considered, namely, the Stokes flow in the leaky-lid cavity, discretized now with a mesh of 20×20 Q_1 elements as in the previous example. In this case, (61) and (62) are solved, with $\boldsymbol{f} = \boldsymbol{0}$, $\nu = 1$, $\bar{\boldsymbol{u}} = (1,0)$ as boundary condition on $y = 1$ ($\bar{\boldsymbol{u}} = \boldsymbol{0}$ on the rest of the boundary), and two different vectors $\boldsymbol{a}$. The pressure contours for $\boldsymbol{a} = (0,0)$ (standard Stokes problem) are shown in Fig. 5 and for $\boldsymbol{a} = (100,0)$ (Oseen equations) in Fig. 6. In both cases, results are more 'diffusive' using the ASGS method. This is observed from the pressure peaks indicated in Table 1 as well as from the curvature of the iso-pressure lines near the boundary, which in the ASGS case tend to be orthogonal to it.

It has to be remarked that, even though there are significant differences in the pressure results, the velocity fields using the ASGS and the OSS methods are very similar.

6.3. Convergence test for the Navier–Stokes equations

In this final example we check the convergence properties of the scheme presented in Section 5.2 when the solution of the continuous Navier–Stokes problems (61) and (62) (now with $\boldsymbol{a} = \boldsymbol{u}$) is smooth. We

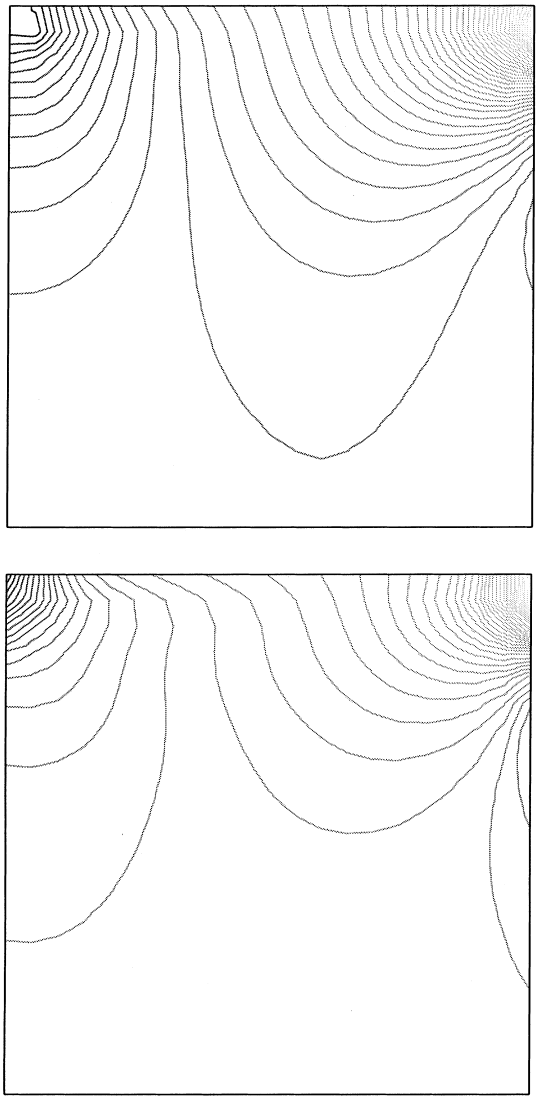

Fig. 6. Pressure contours for the Stokes problem with $\boldsymbol{a} = (100, 0)$. Top: ASGS; bottom: OSS.

Table 1
Comparison of the pressure peaks using the ASGS and the OSS methods

Method	$\boldsymbol{a} = (0, 0)$	$\boldsymbol{a} = (100, 0)$
ASGS	19.698/ − 19.698	58.365/ − 22.168
OSS	38.029/ − 38.029	89.076/ − 44.243

anticipate that, contrary to the previous two cases considered, both the ASGS and the OSS methods have a similar performance.

We take Ω as the unit square and the force term so that the exact solution is $p = 0$ and $\boldsymbol{u}(x, y) = (f(x)g'(y), -f'(x)g(y))$, with $f(x) = x^2(1-x)^2$ and $g(y) = y^2(1-y)^2$. This velocity field vanishes on $\partial\Omega$. The viscosity has been taken $\nu = 0.001$. We have used meshes with different element sizes h, which once normalized range from 0.1 to 0.025. The resulting values of the element Reynolds number are not very high and for this particular example the standard Galerkin approach using a stable velocity–pressure pair

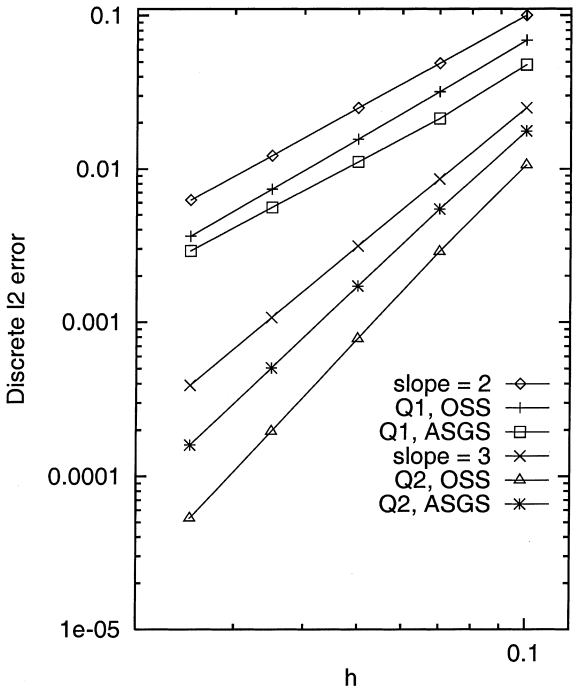

Fig. 7. Discrete ℓ^2 errors for Example 3 using Q_1 and Q_2 elements.

works. Although not shown, results for the Stokes problem turn out to be very similar to those presented below.

In Fig. 7 we have plotted the convergence of the velocities obtained with the OSS and the ASGS methods as the mesh is refined in the discrete ℓ^2 norm and for both the Q_1 (bilinear) and Q_2 (biquadratic) interpolations (with the same set of nodes in both cases). This error is defined as

$$E = \left[\sum_{a=1}^{n_{\text{pts}}} \sum_{i=1}^{2} \left(U_i^a - u_i(\boldsymbol{x}^a) \right)^2 \right]^{1/2} \left[\sum_{a=1}^{n_{\text{pts}}} \sum_{i=1}^{2} \left(u_i(\boldsymbol{x}^a) \right)^2 \right]^{-1/2},$$

where n_{pts} is the total number of nodal points, U_i^a the ith component of the nodal velocity at node a and $\boldsymbol{x}^a$ are the coordinates of this node.

The optimal convergence rate that should be expected is 2 for Q_1 elements and 3 for the Q_2 case. From Fig. 7 it is seen that this is approximately what has been found. For Q_1 elements the absolute error of the ASGS method is smaller than for the OSS, whereas for Q_2 elements the situation is the opposite. In both cases the convergence rate is slightly higher for the OSS method.

7. Conclusions

In this paper, we have introduced a particular sub-grid scale method, which consists of taking as space for the sub-scales the orthogonal to the finite element space. Let us recall once more that the bottom line is to introduce as stabilizing term

$$-\int_{\Omega'} \mathscr{L}^*(\boldsymbol{V}_h)^{\mathrm{t}} \boldsymbol{\tau} P_{h,3} \mathscr{L}(\boldsymbol{U}_h)\, \mathrm{d}\Omega = -\int_{\Omega'} \mathscr{L}^*(\boldsymbol{V}_h)^{\mathrm{t}} \boldsymbol{\tau} [\mathscr{L}(\boldsymbol{U}_h) - P_{h,12} \mathscr{L}(\boldsymbol{U}_h)]\, \mathrm{d}\Omega,$$

where $P_{h,12}$ is the orthogonal projection onto $\mathscr{W}_h$ (finite element space without boundary conditions).

The most important features of this method are the following:

- It has allowed us to recast within the sub-grid scale framework the stabilization of the Stokes problem based on the pressure gradient projection presented in [1]. Recall that this method was originally designed to explain the stabilization properties of some fractional step methods for the transient Navier–Stokes equations. Therefore, the sub-grid scale concept embraces also the stabilization effect of these techniques. It is likely that it will serve to unify other stabilization strategies within the same concept.
- The convergence analysis of the method (see [1] for the Stokes problem and Section 5 for the convection–diffusion–reaction equation) shows that its convergence properties are optimal (in global norms).
- The OSS method is less robust than the ASGS when dealing with sharp boundary layers not parallel to the advection velocity. Numerical experiments have shown that local overshoots near these boundaries are stronger using the first method (this, however, is not necessarily a bad result).
- Related to the previous item, the treatment of boundary values of the unknown is more 'consistent' for the OSS method that for the ASGS one. This is due to the fact that it does not rely on the element residual, which has a low order of approximation near boundaries. In particular, pressure boundary values for incompressible flows are better treated with the OSS method.
- For smooth solutions, the OSS and the ASGS have a similar numerical performance. The former is more expensive as it needs to deal with the projection of certain terms. However, there is no need to compute (and store!) second derivatives to obtain a consistent formulation when higher order interpolations are employed. Moreover, for transient problems the projection onto the finite element space can be done explicitly [18]. This makes the OSS especially appealing when dealing with these transient problems.

References

[1] R. Codina, J. Blasco, A finite element formulation for the Stokes problem allowing equal velocity–pressure interpolation, Computer Methods in Applied Mechanics and Engineering 143 (1997) 373–391.

[2] T.J.R. Hughes, Multiscale phenomena: Green's function, the Dirichlet-to-Neumann formulation, subgrid scale models, bubbles and the origins of stabilized formulations, Computer Methods in Applied Mechanics and Engineering 127 (1995) 387–401.

[3] R. Codina, On stabilized finite element methods for linear systems of convection–diffusion–reaction equations, Computer Methods in Applied Mechanics and Engineering 188 (2000) 61–82.

[4] F. Brezzi, M. Fortin, Mixed and Hybrid Finite Element Methods, Springer, New York, 1991.

[5] R. Codina, O. Soto, Finite element solution of the Stokes problem with dominating Coriolis force, Computer Methods in Applied Mechanics and Engineering 142 (1997) 215–234.

[6] L.P. Franca, T.J.R. Hughes, Convergence analyses of Galerkin least-squares methods for advective–diffusive forms of the Stokes and incompressible Navier–Stokes equations, Computer Methods in Applied Mechanics and Engineering 105 (1993) 285–298.

[7] A.J. Chorin, Numerical solution of the Navier–Stokes equations, Mathematics of Computation 22 (1968) 745–762.

[8] R. Temam, Sur l'approximation de la solution des équations de Navier–Stokes par la méthode des pas fractionaires (I), Archives for Rational Mechanics and Analysis 32 (1969) 135–153.

[9] O.C. Zienkiewicz, R. Codina, A general algorithm for compressible and incompressible flow – Part I. The split characteristic-based scheme, International Journal for Numerical Methods in Fluids 20 (1995) 869–885.

[10] R. Rannacher, On Chorin's projection method for incompressible Navier–Stokes equations, Lecture Notes in Mathematics, vol. 1530, Springer, Berlin, 1992, pp. 167–183.

[11] C. Baiocchi, F. Brezzi, L.P. Franca, Virtual bubbles and Galerkin/least-squares type methods (Ga.L.S), Computer Methods in Applied Mechanics and Engineering 105 (1993) 125–141.

[12] F. Brezzi, L.P. Franca, T.J.R. Hughes, A. Russo, $b = \int g$, Computer Methods in Applied Mechanics and Engineering 145 (1997) 329–339.

[13] R. Codina, A stabilized finite element method for generalized stationary incompressible flows, Computer Methods in Applied Mechanics and Engineering, in press.

[14] R. Codina, M. Cervera, E. Onate, A penalty finite element method for non-Newtonian creeping flows, International Journal for Numerical Methods in Engineering 36 (1993) 1395–1412.

[15] L. Franca, S.L. Frey, T.J.R. Hughes, Stabilized finite element methods: I. Application to the advective–diffusive model, Computer Methods in Applied Mechanics and Engineering 95 (1992) 253–276.

[16] Th. Apel, G. Lube, Anisotropic mesh refinement in stabilized Galerkin methods, Numerische Mathematik 74 (1996) 261–282.

[17] T. Chacón, A term by term stabilization algorithm for the finite element solution of incompressible flow problems, Numerische Mathematik 79 (1998) 283–319.

[18] R. Codina, J. Blasco, Stabilized finite element method for the transient Navier–Stokes equations based on a pressure gradient projection, Computer Methods in Applied Mechanics and Engineering 182 (2000) 287–300.